[Journal of the Arkansas Academy of Science](https://scholarworks.uark.edu/jaas)

[Volume 51](https://scholarworks.uark.edu/jaas/vol51) [Article 13](https://scholarworks.uark.edu/jaas/vol51/iss1/13)

1997

Electron Shock Waves: Effect of Current on Electron Temperature and Density

Mostafa Hemmati
Arkansas Tech University

Mathues Shane Doss
Arkansas Tech University

Electron Shock Waves: Effect of Current on Electron Temperature and Number Density

Mostafa Hemmati and Mathues Shane Doss
Physical Science Department
Arkansas Tech University
Russellville, Arkansas 72801

Abstract

In our attempt to find analytical solutions for breakdown waves, we employ a set of three-component fluid equations. In addition to reporting the method of integration of electron fluid dynamical equations through the dynamical transition region (sheath region), the wave profile for ionization rate, electron number density and electron temperature inside the sheath will be discussed. Also, the effect of the current on electron temperature, electron number density and ionization rate will be reported.

Introduction

For theoretical investigation of breakdown waves a one-dimensional, steady-state, three-component fluid model with a shock front driven by electron gas partial pressure was first presented by Paxton and Fowler (1962). In their model they considered both photoionization and electron impact ionization as important ionization processes. In the fluid model the basic set of equations consists of equations of conservation of mass, momentum, and energy, coupled with Poisson's equation. The system of equations is based on the interactions of three fluids: neutral particles, ions, and electrons. The lack of an experimentally observed Doppler shift in the spectrum of the emitted radiation indicates that in the laboratory the ions and neutral particles have no substantial motion. The fluid phenomenon, therefore, must be due to electron fluid motion alone. Paxton's approximate solutions had a limited success.

Paxton's model was later expanded and modified by Shelton and Fowler (1968). To describe the breakdown waves, Shelton and Fowler (1968) used the terms proforce and antiforce waves, depending on whether the applied electric field force on electrons was with or against the direction of wave propagation. For example, return strokes of lightning flashes are referred to as antiforce waves. Shelton's modified version used frame invariance to find analytic forms for elastic and inelastic collision terms, and the ionization was considered to be due to electron impact only. Shelton's approximation methods in solving the electron fluid equations with "certain limiting conditions governing the existence of such steady-profile waves" had relatively good agreement with experimental results in the allowed limited range of wave speeds.

Following Fowler's (1976) classification, the breakdown waves propagating into a nonionized medium will be referred to as Class I waves, those moving into a preionized medium will be called Class II waves, and the waves for which a large electric current exists behind the shock front will be referred to as Class III waves. If a contained volume of plasma is subjected to an electric field, a Debye sheath layer will form. Excess charges of one polarity create a space charge field in the layer which cancels out the applied field. The interior region of the plasma, therefore, is essentially field free and neutral. The thin Debye region in which the field falls to a negligible value and the electrons come to rest relative to the heavy particles, will be referred to as the sheath region.

Theory and Model

In the one-dimensional model of electrical discharges, assuming that the electric field is in the direction of the negative x-axis (proforce waves), the electric field force on electrons will be in the direction of the positive x-axis. In the neighborhood of the pulsed electrode, the electric field is very large and intense ionization takes place. The field accelerates the free electrons until they attain enough energy for collisional ionization of the gas. The intense electric field, the highest intensity of which is considered to be at the interface between the neutral gas and the ionized gas, causes the continuation of this process and forward motion of the interface into the neutral gas. For ionizing waves (also referred to as potential waves), the interface is a shock front.

The shock front in breakdown waves is followed by a dynamical transition region. The transition region, which is somewhat thicker than a Debye length will be referred to as the sheath region. In the sheath region electrons come to rest relative to neutrals, and the net electric field falls to zero at the trailing edge of the sheath. The large difference in electron and ion mobility results in the establishment of space charge and therefore, of a space charge field inside the sheath. The net electric field is the sum of the applied field and the space charge field. The sheath region is followed by a relatively thicken quasi-neutral region in which the electron gas heated in the sheath region cools off by further ionizing the neutral particles. In the wave frame, an observer traveling with the wave will see a cold gas enter the sheath region from the front while a partially ionized gas leaves the rear side of the sheath. For breakdown waves to advance without significant damping, during ionization inside the sheath the change of electron fluid momentum must be small compared to the force due to the electron gas pressure gradient. The electron gas partial pressure, therefore, is considered to provide the driving force in the fluid dynamical analysis of the ionizing waves.

In our attempt to find analytical solutions, we will employ a set of three-component fluid equations which were completed by Fowler et al. (1984). They have reduced their original system of twelve electron fluid equations (continuity, momentum, and energy conservation) in tensor notations to a single system of nonlinear differential equations. Their system of electron-fluid equations plus Poisson's equation for breakdown of ionless media, respectively, are

$$\frac{d(nv)}{dx} = \beta n. \qquad (1)$$

$$\frac{d}{dx}\left\{ nmv(v - V) + nkT_e \right\} = -enE - Kmn \ (v - V). \qquad (2)$$

$$\frac{d}{dx}\left\{ nmv(v - V)^2 + nkT_e \ (5v - 2V) + 2e\phi nv + \epsilon_0 VE^2 - \frac{5nk^2 \ T_e}{mk}\frac{dT_e}{dx} \right\}$$

$$= -3\left(\frac{m}{M}\right) nkKT_e - mnK \ \left(\frac{m}{M}\right)(v - V)^2. \qquad (3)$$

$$\frac{dE}{dx} = \frac{en}{\epsilon_0}\left(\frac{v}{V} - 1\right). \qquad (4)$$

The symbols m, e, n, and T_e represent electron mass, charge, number density, and temperature inside the sheath, and K, β, φ, V, M, E_0, x are elastic collision frequency, ionization frequency, ionization potential, wave velocity, neutral particle mass, electric field at the wave front, and position inside the sheath, respectively.

Analysis

The analysis will partially involve the use of methods similar to those employed by Fowler et al. (1984). Introducing dimensionless variables

$$\theta = \frac{kT_e}{2e\phi}, \quad \eta = \frac{E}{E_0}, \quad \xi = \frac{eE_0}{mV^2}x, \quad \psi = \frac{v}{V}, \quad \omega = \frac{2m}{M}, \quad \kappa = \frac{mVK}{eE_0},$$

$$\mu = \frac{\beta}{K}, \quad \alpha = \frac{2e\phi}{mV^2}, \quad \nu = \frac{2e\phi}{\epsilon_0 E_0^2}n$$

into the system of electron-fluid equations, one can achieve nondimensionalization of the equation set.

$$\frac{d(\nu\psi)}{d\xi} = \kappa\mu\nu,$$

$$\frac{d}{d\xi}\left\{\nu\psi(\psi - 1) + \alpha\nu\theta\right\} = -\nu\eta - \kappa\nu(\psi - 1),$$

$$\frac{d}{d\xi}\left\{\nu\psi(\psi - 1)^2 + \alpha\nu\theta(5\psi - 2) + \alpha\nu\psi + \alpha\eta^2 - \frac{5\alpha^2\nu\theta}{\kappa}\frac{d\theta}{d\xi}\right\} = -\omega\kappa\nu\left\{3\alpha\theta + (\psi - 1)^2\right\},$$

$$\frac{d\eta}{d\xi} = \frac{\nu}{\alpha}(\psi - 1).$$

In the above equations, ν, ψ, θ, μ, κ, η, and ξ are the dimensionless electron concentration, electron velocity, electron temperature, ionization rate, elastic collision frequency, electric field, and position inside the sheath, respectively.

For proforce current bearing waves (Class 111 waves) to integrate the set of electron-fluid-dynamical equations through the sheath region, we will use Hemmati and Young's (1995) modified Poisson's equation and their equation for electron temperature at the shock front. The two equations have proven to be successful in solving the problem, and they, respectively, are

$$\frac{d\eta}{d\xi} = \frac{\nu}{\alpha}(\psi - 1) + \kappa\iota, \qquad (9)$$

$$\theta_1 = \frac{\psi_1(1 - \psi_1)}{\alpha} + \frac{\kappa}{\nu_1}\iota, \qquad (10)$$

where $\iota = \frac{I_1}{\epsilon_0 E_0 K_1}$, with I_1 as the current behind the shock front.

In a review of the present understanding of lightning, Uman (1993) identifies four different types of lightning between cloud and Earth. A typical cloud-to-ground lightning flash starts with a "step leader" which then propagates down from the top in quantized steps of about 50 meters in length. Leader steps have a duration of 1 μs and pause time of approximately 20 to 50 μs. The total time elapsed until the step leader touches the ground is approximately tens of milliseconds, and its average speed is about 2 x 10^5 m/s. Following the last step, a very bright wave containing a large amount of charge moves very quickly from the ground to the cloud. This is referred to as the return stroke. The duration of time elapsed until the return stroke traverses the length of the previously charged leader channel is on the order of 100 μs, and it has a speed roughly one-third the speed of light. After a period of tens of milliseconds, if additional charge is available at the bottom of the cloud, a wave propagates smoothly from the cloud to the ground along the first-stroke channel. This wave is referred to as the dart

Journal of the Arkansas Academy of Science, Vol. 51 [1997], Art. 13

leader, and it will be followed by a new return stroke. From observations on twenty-one dart leaders, Orville and Idone (1982) report total distances in the range of 3.5 – 17.2 km, speeds in the range of 2.9 to 23 x 10^6 m/s, and average dart length of 34 m. The dart leader lowers a total charge on the order of 1 C during a total time on the order of 1 ms.

Allowing lightning discharge to pass through fiberglass screen, Uman (1964) has been able to determine the diameter of the lightning stroke. Considering the diameter of the inner core as the diameter of the lightning, his measurements resulted in values in the range of 2 to 3.5 cm for the diameter of the lightening stroke. For a dart leader carrying electron number density of n ~ 10^{13} e/cm^3 (Fowler, 1964) with a channel radius of r ~ 2 cm, and propagation speed of v ~ 10^6 m/s, one can calculate the approximate value of conduction current from the equation I = nevA to be I ~ 2000 A. Similar calculations of the current in a stepped leader will result in an average value of 500 A, and peak current value of 30 KA for a return stroke.

The value of the dimensionless current, ι, depends on the choice of values of electric field at the wave front, E_0, and elastic collision frequency , K, where both are scaled with electron pressure. Using the appropriate values of K for nitrogen and with current magnitudes calculated in the last paragraph, the value of ι will be on the order of 0.005–0.1.

The first objective of this paper is the integration of the electron-fluid dynamical equations for proforce Class III waves. To achieve integration of the set of equations through the sheath region, one has to place the singularity inherent in the equation system in the denominator of the momentum integral (Fowler et al., 1984).

$$\frac{d\psi}{d\xi} = \frac{\kappa\psi(1+\mu)(1-\psi) - \alpha\theta\kappa\mu - \alpha\psi\theta' - \eta\psi}{\psi^2 - \alpha\theta}. \qquad (11)$$

A zero denominator in the momentum integral represented an infinite value for the electron velocity derivative with respect to the position inside the sheath. This condition requires the existence of a shock inside the sheath region, which is not allowed. The numerator in the momentum integral, therefore, has to become zero at the same time that the denominator becomes zero. For a given wave speed in the process of integration of the equations through the sheath region, comparing the numerator and denominator values will allow one to choose the required initial parameters (ν_1, ψ_1, and κ) by trial and error. A successful solution has to allow passage through the singularity and satisfy the physically acceptable conditions at the trailing edge of the sheath. The expected conditions at the end of the sheath are, a) the electrons have to come to rest relative to neutral particles ($\psi \rightarrow 1$), and b) the net electric field has to reduce to a negligible value ($\eta \rightarrow 0$). Our solutions satisfy the expected boundary conditions at the trailing edge of the wave within the accuracy of the integration step.

All the current values which allow for the integration of the set of electron-fluid equations through the sheath region have been investigated. This has resulted in a theoretically calculated current range using electron fluid approach. The prepared successful current range (ι = 0.001 ~ 0.5) compares well with the range of current values calculated in this paper and current ranges measured by a number of researchers. This agreement on current range is another confirmation on the validity of the electron-fluid model for electrical discharge of gases. The following are several articles with different methods of current measurements or calculations.

In two succeeding articles Uman and McLain were able to derive expressions relating the current in lightning to the radiation field (electric field intensity or magnetic flux density). In their first article (Uman and McLain, 1970a), their calculated value of the peak current for the typical stepped leader waveform described by Pierce was between about 800 A and 5 KA. The derived expressions in their second article (Uman and McLain, 1970b) allowed them to calculate the current in a lightning return stroke from a measurement of the radiation field. They reported a typical stepped leader peak field of about 1/20 of the peak field of a typical return stroke at 100 Km. In analyzing the data, they assumed that the ratio of the peak fields is proportional to the ratio of the maximum rates of change of current. In a separate article, "Comparing Lightning and Long Laboratory Spark for Stepped Leader," Uman (1971) reports an average current of 100 A and a peak current of 1000 A. Treating the current behind the wave front as a switch-on transient in a transmission line, Little (1978) was able to model and calculate the variation of current in a return stroke with altitude. His calculated value of the average peak current in the stroke is roughly 88 KA.

Results

The integration of the system of electron fluid dynamical equations provides variations on electron temperature, electron number density and ionization rate within the sheath region. In our investigation, the current values selected were 0.001, 0.01, 0.1, 0.25, and 0.5. We were able to integrate the system of equations through the sheath region even for current value as high as 0.5. For ι = 0.5, however, the passage through the singularity required keeping the numerator and denominator in the momentum integral constant up to 25 integration steps. This results in a kink in the graphs when variables such as θ, ν, and μ are plotted. Our graphs, therefore, include current values up to 0.25.

We have integrated the system of electron fluid dynamical equations for a fast moving wave ($\alpha = 0.01$, $V = 3 \times 10^7$ m/s). Figure 1 is a plot of electric field, η, as a function of electron velocity, ψ, inside the sheath. For all current values, the results meet the expected boundary conditions at the end of the sheath ($\eta \rightarrow 0$, $\psi \rightarrow 1$). Figure 2 is a plot of electron temperature, θ, as a function of position, ξ, inside the sheath. The results conform with the expected variations of the electron temperature within the sheath. For all current values, the electron gas temperature decreases near the end of the sheath.

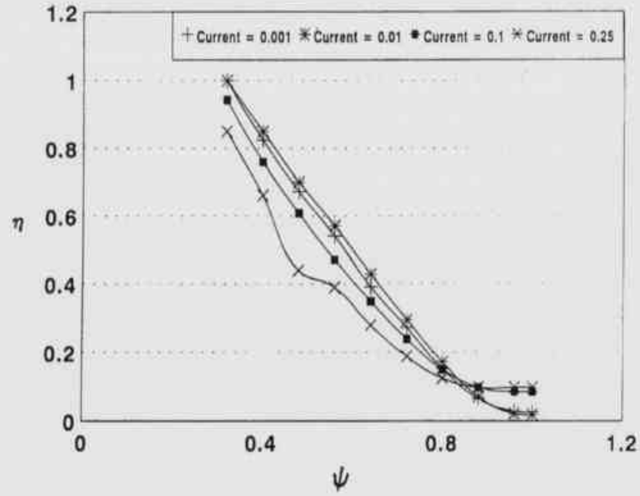

Fig. 1. Electric field, η, as a function of electron velocity, ψ, inside the sheath.

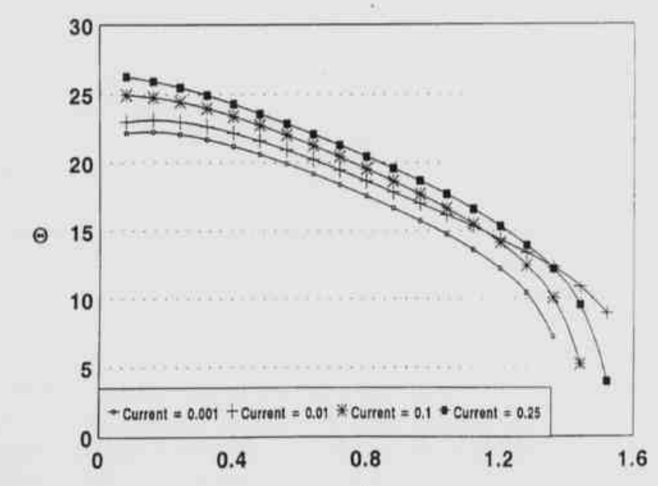

Fig. 2. Electron temperature, θ, as a function of positions ξ, inside the sheath.

Figure 3 is a graph of electron number density, ν, as a function of position inside the sheath. For current value of 0.25, the passage through the singularity requires a higher level of approximation and therefore, provides a kink in the graph of electron number density as a function of position, ξ.

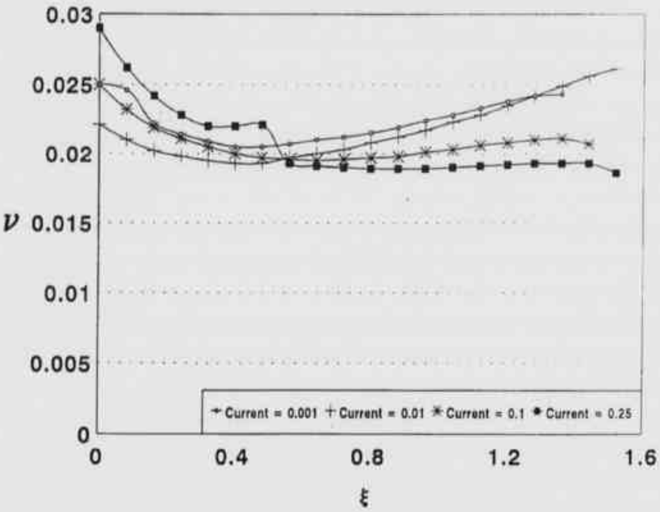

Fig. 3. Electron number density, υ, as a function of position, ξ, inside the sheath.

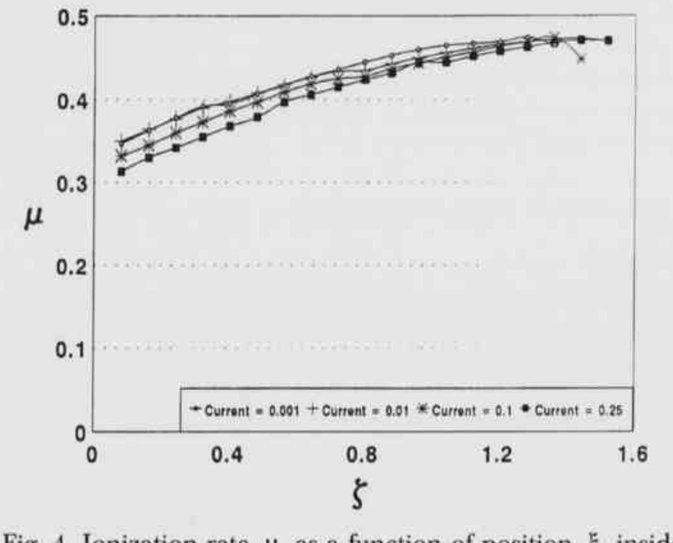

Fig. 4. Ionization rate, μ, as a function of position, ξ, inside the sheath.

Figure 4 represents the variation of ionization rate, μ, as a function of position inside the sheath. The earlier assumption, that the ionization rate throughout the region where electric field is present was held constant, has been replaced by using a double integral to calculate it [Fowler et al. (1984)]. As Fig. 4 indicates, the ionization rate derived, based on the directed as well as random motion of electrons, changes within the sheath region.

Conclusions

As Fig. 4 indicates, for all current values the ionization rate increases near the trailing edge of the sheath. This is due to high electron temperatures which make further ionization possible. The results indicate that the sheath thickness is effected by the changes in the value of the current behind the shock front. As the current increases the sheath thickness also increases slightly. Solutions for smaller wave propagation speeds are possible; however, the integration of the set of electron fluid equations become more difficult as the wave speed decreases.

ACKNOWLEDGMENTS.—The authors would like to express their gratitude to the Arkansas Space Grant Consortium for its financial support of this research project.

Literature Cited

Fowler, R.G. 1964. Electrons as a hydrodynamical fluid. Adv. Electronics and Electron Phys. 20:1-58.

Fowler, R.G. 1976. Nonlinear electron acoustic waves, Part II. Adv. in Electronics and Electron Physics. 41:1-72.

Fowler, R.G., M. Hemmati, R.P. Scott, and **Parsenajadh.** 1984. Electric breakdown waves: Exact numerical solutions. Part I. Phys. Fluids. 27:1521-1526.

Hemmati, M. and **S. Young.** 1995. Proforce waves: The effect of current behind the shock front on wave structure. Proc. Arkansas Acad. Sci. 49:56-59.

Little, P.F. 1978. Transmission line representation of a lightning return stroke. J. Phys. D. 11:1893-1910.

Orville, R.E. and **V.P. Idone.** 1982. Lightning leader characteristics in the Thunderstorm Research International Program (TRIP). J. Geophys. Res. 87:11117-11192.

Paxton, G.W. and **R.G. Fowler.** 1962. Theory of breakdown wave propagation. Phys Rev. 128:993-997.

Shelton, G.A. and **R.G. Fowler.** 1968. Nature of electron-fluid-dynamical waves. Phys. Fluids. 11:740-746.

Uman, M.A. and **D.K. McLain.** 1970a. Radiation field and current of the lightning stepped leader. J. Geophys. Res. 75:1058-1066.

Uman, M.A. and **D.K. McLain.** 1970b. Lightning return stroke current from magnetic and radiation field measurements. J. Geophys. Res. 75:5143-5147.

Uman, M.A. 1964. The diameter of lightning. J. Geophys. Res. 69:583-585.

Uman, M.A. 1971. Comparison of lightning and long laboratory spark. Proc. IEEE 59:457-466.

Uman, M.A. 1993. Natural Lightning. Proc. IEEE Industrial and Commercial Power Systems Technical Conference. Vol. 93ch3255-7 pp. 1-7.